

Dynamic Spin Ice: $\text{Pr}_2\text{Sn}_2\text{O}_7$

H. D. Zhou,^{1,2} C. R. Wiebe,^{1,2,*} J. A. Janik,^{1,2} L. Balicas,² Y. J. Yo,² Y. Qiu,^{3,4} J. R. D. Copley,³ and J. S. Gardner^{3,5}

¹Department of Physics, Florida State University, Tallahassee, Florida 32306-3016, USA

²National High Magnetic Field Laboratory, Florida State University, Tallahassee, Florida 32306-4005, USA

³NIST Center for Neutron Research, Gaithersburg, Maryland, 20899-8102, USA

⁴Department of Materials Science and Engineering, University of Maryland, College Park, Maryland, 20742, USA

⁵Indiana University, 2401 Milo B. Sampson Lane, Bloomington, Indiana 47408, USA

(Received 13 April 2008; published 26 November 2008)

In this Letter, we report a new spin ice— $\text{Pr}_2\text{Sn}_2\text{O}_7$ —which appears to have enhanced residual entropy due to the dynamic nature of the spins. Neutron scattering experiments show that at 200 mK, there is a significant amount of magnetic diffuse scattering which can be fit to the dipolar spin-ice model. However, these short-ranged ordered spins have a quasielastic response that is atypical of the canonical spin ices, and suggests that the ground state is dynamic (i.e., composed of locally ordered two-in–two-out spin configurations that can tunnel between energetically equivalent orientations). We report this as an example of a *dynamic* spin ice down to 200 mK.

DOI: 10.1103/PhysRevLett.101.227204

PACS numbers: 75.50.Lk, 75.25.+z, 75.40.–s, 78.70.Nx

The pyrochlores, denoted by the formula $A_2B_2O_7$, belong to a special class of geometrically frustrated materials that have provided the condensed matter community with a plethora of interesting ground states, ranging from spin liquid through spin glass through spin-ice behavior. In the cases where the *A* site is occupied by a rare-earth-metal element, strong-crystal-field effects play a role in this rich behavior [1]. At low temperatures, the magnetic properties are controlled by the magnetic exchange (J_{NN}) and dipolar interaction (D_{NN}) of the nearest-neighbor spins [2]. In general, when the exchange interactions tend to be antiferromagnetic in nature, and much stronger than the dipolar interactions, then unusual magnetic states flourish due to the inherent frustrated sublattice. In the case where the exchange energy scale is small compared to the dipolar energy scale, long-ranged ordered states tend to prevail.

Spin ices are a very special case. In general, the spin-ice ground state tends to occur when both J_{NN} and D_{NN} are of comparable energy scales [3]. As well, there must be sufficient uniaxial anisotropy induced on the rare-earth site from crystal-field interactions to render the spins to be Ising-like with only two possible orientations along the $\langle 111 \rangle$ direction. If these conditions are satisfied, the system cannot order through minimizing the dipolar interactions alone—a short-ranged ordered state develops. In the case where there is weak ferromagnetism, the spins upon each tetrahedron freeze out into local two-in–two-out configurations. This has a direct analogy to the two-short–two-long proton bond disorder about each oxygen atom in water ice, hence the name “spin ice.” In fact, the calculation of the low-temperature entropy in water ice can be mapped onto the spin-ice problem to yield $S = R[\ln 2 - \frac{1}{2} \ln(\frac{3}{2})]$ [4–6]. This gives a zero point entropy as $\frac{1}{2} R \ln(\frac{3}{2})$, which is the same as predicted by Pauling for ice [7]. Until now, the studied spin-ice systems, the rare-earth

titanates $\text{Ho}_2\text{Ti}_2\text{O}_7$ [4] and $\text{Dy}_2\text{Ti}_2\text{O}_7$ [6], all have rare-earth elements with large magnetic moment. This means that there is a strong dipolar interaction in the system due to the large moment: $D_{\text{NN}} = \frac{5}{3}(\mu_0/4\pi)\mu^2/r_{\text{NN}}^3$ (r_{NN} is the nearest-neighbor for pyrochlore) [2]. There are no examples in the literature of spin-ice states found in pyrochlores beyond the Ho^{3+} and Dy^{3+} sublattices.

According to the phase diagram presented by den Hertog and Gingras, spin-ices states should be stable for a wide range of D_{NN} and J_{NN} values [3]. Over several decades, the rare-earth titanates and stannates have been characterized to search for unusual ground states such as the spin ice. In many cases, either the crystal-field interactions, or the size of the exchange term, or the nature of the local spin interactions disturbs the realization of a spin ice beyond the Ho^{3+} or Dy^{3+} members. An even greater problem is the loss of stability of the pyrochlore structure—at ambient pressure, $\text{Pr}_2\text{Ti}_2\text{O}_7$, for example, has a monoclinic structure instead of cubic [8]. But by substituting nonmagnetic Sn^{4+} for Ti^{4+} , one can synthesize the pyrochlore $\text{Pr}_2\text{Sn}_2\text{O}_7$. The DC susceptibility of this sample shows that the sample has an Ising magnetic anisotropy along the trigonal axis and ferromagnetic coupling [9]. There is also evidence that the ground state is a doublet, with a well-separated energy gap to the next energy state of at least 100 K. These results suggest a potential spin-ice ground state in $\text{Pr}_2\text{Sn}_2\text{O}_7$, but until now, experimental evidence for this has been lacking. Here, we present detailed specific heat and neutron scattering measurements on $\text{Pr}_2\text{Sn}_2\text{O}_7$ to show that a dynamic spin-ice state emerges at low temperatures.

Polycrystalline samples of $\text{Pr}_2\text{Sn}_2\text{O}_7$ were made by a standard solid state reaction. DC susceptibility measurements were made with a SQUID magnetometer. The specific heat measurements were made with a physical

property measurement system. Neutron scattering measurements were completed at the NIST CHRNS using the Disk Chopper Spectrometer (DCS) with wavelengths of 2.3, 5.0, and 9.0 Å.

The lattice parameter for our sample agrees well with other reports in the literature [9]. The DC magnetic susceptibility [$\chi(T)$] of $\text{Pr}_2\text{Sn}_2\text{O}_7$, inset of Fig. 1(a), shows no signs of conventional magnetic ordering down to 1.8 K and a Weiss temperature of $\theta_{\text{CW}} = 0.3$ K consistent with previous work. The specific heat data, $C_p(T)$, also shows no evidence of magnetic long-ranged order down to 0.37 K. The magnetic specific heat $C_{\text{mag}}(T)$ is obtained after subtraction of a nonmagnetic lattice contribution [$C_p(T)$ of $\text{La}_2\text{Sn}_2\text{O}_7$]. C_{mag}/T exhibits a broad peak at $T_{\text{peak}} = 0.86$ K, characteristic of the short-ranged ordering observed in spin ices. The integration of C_{mag}/T gives an entropy of $S_{\text{mag}} = 3.1$ J/mol_{Pr} K, which is recovered to 4.8 J/mol_{Pr} K with an applied magnetic field of $\mu_0 H = 1$ T.

One important aspect to test the validity of a spin-ice-like state is to determine the nature of the crystalline electric field about the Pr ions. In a crystalline electronic field (CEF) with symmetry D_{3d} for the cubic pyrochlore, the ninefold degenerate ground state 3H_4 of the Pr^{3+} ion splits into 3 doublets and 3 singlets. The susceptibility measurements on $\text{Pr}_2\text{Sn}_2\text{O}_7$ suggest that the CEF ground state is a non-Kramers doublet, and has the correct Ising-like anisotropy along the $\langle 111 \rangle$ axis [9]. Other Pr-based pyrochlores show a similar crystal-field energy scheme

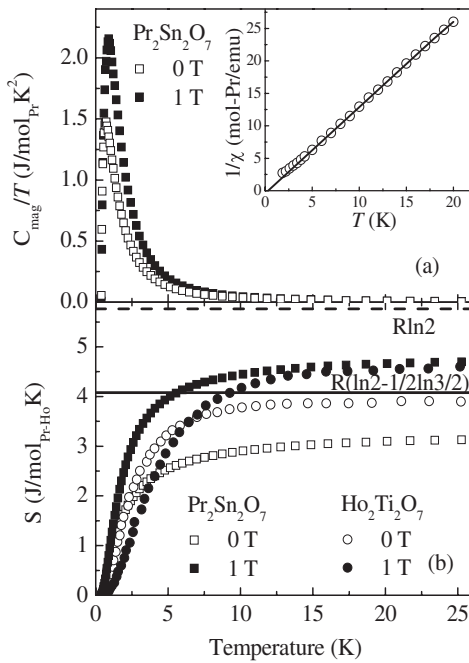


FIG. 1. (a) C_{mag}/T of $\text{Pr}_2\text{Sn}_2\text{O}_7$ in $\mu_0 H = 0$ and 1 T; Inset: Susceptibility of $\text{Pr}_2\text{Sn}_2\text{O}_7$ in $\mu_0 H = 1$ T. (b) Entropy of $\text{Pr}_2\text{Sn}_2\text{O}_7$ and $\text{Ho}_2\text{Ti}_2\text{O}_7$.

[10]. Our higher energy inelastic scattering spectra ($\lambda = 2.3$ Å) at $T = 200$ K for $\text{Pr}_2\text{Sn}_2\text{O}_7$ [Fig. 2(a)] shows evidence for two nearly dispersionless crystal-field excitations at 19 meV (210 K) and 38 meV (430 K).

Diffraction data taken at $T = 4.6$ K and $T = 0.2$ K show no new Bragg peaks forming at low temperatures [Fig. 2(b)]. However, there is a significant amount of elastic magnetic diffuse scattering [Fig. 2(c) and 2(d)]. The extra diffuse magnetic scattering intensity peaks at approximately $|Q| = 0.5$ Å⁻¹. The cut along $|Q|$ from integrated energies of -0.05 meV $< E < 0.05$ meV shows this feature in more detail.

Figure 3 shows the inelastic neutron scattering spectra for $\text{Pr}_2\text{Sn}_2\text{O}_7$ at 180, 1.4, and 0.2 K. It is clear that a magnetic component is developing upon a nearly temperature independent chemical background. As the temperature decreases, the magnetic signal develops as a strong quasi-elastic component with a shoulder extending to higher energies. The spectra can be fit to a standard Lorentzian form for slow spin excitations:

$$I(E) = A\delta(E) + B \frac{D(E)\Gamma}{\pi(\Gamma^2 + E^2)} \quad (1)$$

where the first term represents the incoherent nuclear scattering and the second term represents the quasielastic magnetic component (A and B are constants). Γ is the half-width of the quasielastic peaks, and the function $D(E)$ is the detailed balance factor. In Fig. 3, the fits of Eq. (1) to

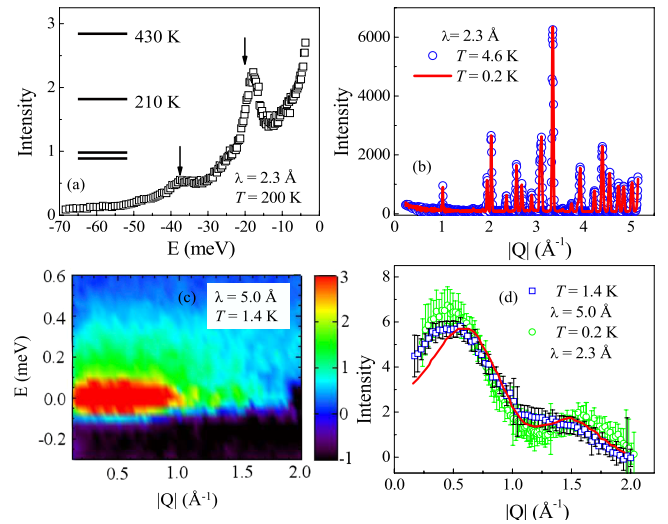


FIG. 2 (color online). (a) Higher energy inelastic scattering integrated over Q ($\lambda = 2.3$ Å) at 200 K showing two broad excitations. A possible crystal-field scheme is illustrated in the inset; (b) Elastic diffraction data at 4.6 and 0.2 K showing no signs of new Bragg peaks; (c) Contour plot of neutron scattering data $S(E, Q)$ ($\lambda = 5.0$ Å) at 1.4 K, the data is obtained by subtracting a 50 K dataset as background; (d) Elastic magnetic diffuse scattering at 1.4 and 0.2 K. The line is a mean field calculation for a typical dipolar spin ice from [12].

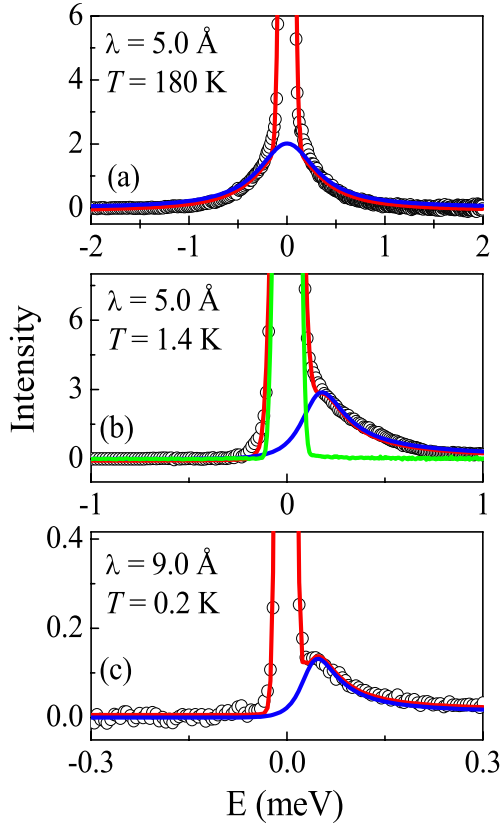


FIG. 3 (color online). Inelastic spectra at (a) 180 K, (b) 1.4 K, and (c) 200 mK. Open circles are experimental data, the two sets of lines in (a) and (c) are the fits to Eq. (1) and the weak quasielastic component. In (b), the spectrum for $\text{Ho}_2\text{Ti}_2\text{O}_7$ at 1.4 K is shown for comparison.

the experimental data are shown, with the magnetic contribution. Note that the magnetic component is offset from $E = 0$ at 1.4 and 0.2 K, which is due to the resolution convolution and the detailed balance factor. The magnetic scattering becomes sharper with decreasing temperature, signalling a general slowing down of the spin dynamics. Figure 4(b) shows the temperature dependence of characteristic relaxation time τ derived from the full-width at half maximum (FWHM) of the quasielastic scattering. For direct comparison, the relaxation time for $\text{Ho}_2\text{Ti}_2\text{O}_7$ is shown in the upper panel [Fig. 4(a)] as derived from inelastic neutron spectroscopy by Ehlers *et al.* [11]. The high temperature response from $\text{Ho}_2\text{Ti}_2\text{O}_7$ only shows an energy barrier of 300 K from crystal-field excitations, whereas $\text{Pr}_2\text{Sn}_2\text{O}_7$ has an anomalous activation barrier of 1.4 K extending over a wide range of temperatures down to below 1 K.

The nearest-neighbor dipolar interaction in $\text{Pr}_2\text{Sn}_2\text{O}_7$ is estimated to be $D_{\text{NN}} = 0.13$ K by using the Pr-Pr distance in the tetrahedra (3.75 Å) and the magnetic moment $2.6\mu_B/\text{Pr}$ [9]. This D_{NN} is almost 20 times smaller than that of the spin ices $\text{Ho}_2\text{Ti}_2\text{O}_7$ and $\text{Dy}_2\text{Ti}_2\text{O}_7$ ($D_{\text{NN}} \sim 2.5$ K). den Hertog and Gingras have elucidated the phase

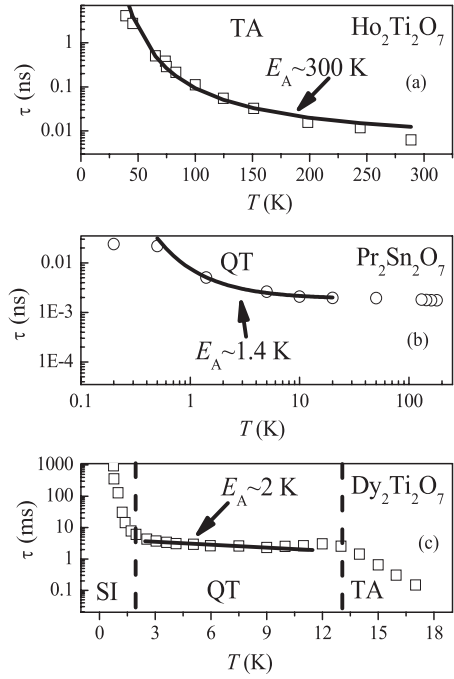


FIG. 4. (a) Temperature dependence of the relaxation time, τ , for (a) $\text{Ho}_2\text{Ti}_2\text{O}_7$ from [11], (b) $\text{Pr}_2\text{Sn}_2\text{O}_7$ extracted from the neutron data via τ (ns) = 1.31/FWHM(μeV) [11], (c) $\text{Dy}_2\text{Ti}_2\text{O}_7$, from [14]. SI: Spin-ice region; QT: Quantum tunneling region; TA: Thermal activation region. The solid lines are fits to the Arrhenius law.

diagram for possible spin ices given the exchange and dipolar interaction energy scales. According to their phase diagram, if the magnetic specific heat shows a peak at 0.86 K, then the ratio of $T_{\text{peak}}/D_{\text{NN}} = 6.6$. If we extend the $J_{\text{NN}}/D_{\text{NN}} T_{\text{peak}}/D_{\text{NN}}$ phase diagram calculated from the Monte Carlo method for the pyrochlore spin ice [3], we obtain $J_{\text{NN}}/D_{\text{NN}} = 7.1$, and therefore $J_{\text{NN}} = 0.92$ K. This value of J_{NN} is reasonable for a small $\theta_{\text{CW}} = 0.3$ K, which is notoriously difficult to measure exactly in the pyrochlore titanates. In $\text{Pr}_2\text{Sn}_2\text{O}_7$, the dipolar interaction energy scale is much weaker than the magnetic exchange energy scale.

Although D_{NN} is weak, the diffuse scattering at 1.4 K for $\text{Pr}_2\text{Sn}_2\text{O}_7$ still shows Q -dependent features: a broad peak at around $|Q| = 0.5 \text{ \AA}^{-1}$ and another small feature at around $|Q| = 1.5 \text{ \AA}^{-1}$ typical for a dipolar spin ice [12]. The line in Fig. 2(d) is from a mean field calculation of the integrated powder intensity profile of a typical spin ice [12]. This calculation reproduces most of the features of our experimental data, but several caveats are noteworthy: (i) it is difficult to determine the exchange and dipolar contributions from powder data, and (ii) it is clear that there is a strong exchange component to the scattering. This is evident through, for example, the enhanced scattering at low- Q due to the ferromagnetic interactions between the moments that have not been added to the dipolar spin-ice model.

One signature of the pyrochlore spin ice is the entropy $S = R[\ln 2 - \frac{1}{2} \ln(\frac{3}{2})] = 4.08$ J/mol K. For $\text{Pr}_2\text{Sn}_2\text{O}_7$, as shown in Fig. 1(b), the calculated entropy at zero field is $S = 3.1$ J/mol_{Pr} K, a shortfall of about 25% of the spin-ice entropy. This indicates that the ground state of $\text{Pr}_2\text{Sn}_2\text{O}_7$ must be more dynamic than that of the known spin ices. With an applied field $\mu_0 H = 1$ T, the entropy of $\text{Pr}_2\text{Sn}_2\text{O}_7$ recovers to 4.8 J/mol_{Pr} K, which is similar to that of the spin ice $\text{Ho}_2\text{Ti}_2\text{O}_7$. The symmetry breaking effect of the magnetic field should be similar for both spin ices and recover the same entropy of the two state system. The magnetic fluctuations which presumably stabilize the ground state in $\text{Pr}_2\text{Sn}_2\text{O}_7$ must be severely quenched in an applied field. The existence of magnetic scattering at low temperature also supports the conjecture of a dynamic low-temperature spin state for $\text{Pr}_2\text{Sn}_2\text{O}_7$. Although the FWHM for $\text{Pr}_2\text{Sn}_2\text{O}_7$ decreases rapidly at low temperatures, the quasielastic peak at 0.200 K still shows a width of 0.100(10) meV (FWHM). For comparison, $\text{Ho}_2\text{Ti}_2\text{O}_7$ [Fig. 3(b)] shows essentially no magnetic quasielastic component using the same instrumental resolution, indicating a static spin state.

The dynamics of spins for the studied spin-ice systems typically goes through three stages with decreasing temperature: a “thermal” activated region at high temperature, a spin freezing region at low temperature, and a quantum tunneling region between them [Fig. 4(c)]. The characteristic feature of the quantum tunneling region is the weak temperature dependence of the relaxation time which results in a small energy barrier on the order of several Kelvin. For example, the relaxation time measured from high resolution inelastic neutron scattering for $\text{Ho}_2\text{Ti}_2\text{O}_7$ [Fig. 4(a)] shows an Arrhenius law at high temperature with energy barrier of around 300 K (governed by the crystal-field excitation energy scale). At low temperatures, the spins become more static, and other techniques such as AC susceptibility are needed to track the behavior. The relaxation time in $\text{Dy}_2\text{Ti}_2\text{O}_7$ is shown in Fig. 4(c) for comparison. Note that there is a plateau region, indicating a weak energy barrier of 2 K, which is associated with the quantum relaxation region beneath 13 K. Then, below 2 K, the relaxation time increases again, which is due to the spin freezing in the spin-ice state [11,13,14]. In comparison, the $\text{Pr}_2\text{Sn}_2\text{O}_7$ data also show a energy barrier of 1.4 K from our fit to the inelastic spectra [Fig. 4(a)] over a wide range of temperatures. These results suggest that $\text{Pr}_2\text{Sn}_2\text{O}_7$ still sits in the quantum tunneling region at least down to 200 mK and does not reach a freezing regime. In fact, the spin fluctuations seem to reach a limit beneath 1 K with a time scale (0.01 ns) which is 9 orders of magnitude faster than $\text{Dy}_2\text{Ti}_2\text{O}_7$. Although the mechanism for this dynamic state is currently unknown, we surmise that a tunneling process between equivalent two-in–two-out spin configurations is the source for this response. Recently, the work of

Matsuhira *et al.* has shown that there is a broad feature in the magnetic susceptibility, followed by a sharp decrease beneath 0.4 K [9]. We have not seen any indication that this is a transition to an ordered state with our data, with little change in the diffuse scattering profile or the diffraction pattern at 0.2 K. However, we do note that our spin fluctuation rate seems to be a constant beneath 0.5 K. Future work is needed to elucidate the slow spin dynamics that must be present at low temperatures.

The ground state of $\text{Pr}_2\text{Sn}_2\text{O}_7$ therefore shows the characteristic elastic neutron scattering profile of a spin ice, but with a highly dynamic inelastic component compared to $\text{Ho}_2\text{Ti}_2\text{O}_7$ or $\text{Dy}_2\text{Ti}_2\text{O}_7$. Our data suggest that down to at least 0.2 K, $\text{Pr}_2\text{Sn}_2\text{O}_7$ appears to have quantum relaxation and an absence of true spin freezing. In the early work on spin ices, magnetic analogues were searched for that had weak ferromagnetism and strong local anisotropy [2], but it is now becoming more apparent that there is a rich spectrum of different “ice-like” compounds which exist in the limit of T approaching 0 K. The “dynamic spin-ice” state in $\text{Pr}_2\text{Sn}_2\text{O}_7$ should provide a fruitful arena for further study of quantum phenomena in solids, such as the recent discovery of monopole formation in “static” spin ice [15], cooperative magnetic excitations seen in pyrochlore spin liquids such as $\text{Tb}_2\text{Ti}_2\text{O}_7$ [16], the nature of the ground state in other spin-ice candidates such as $\text{Tb}_2\text{Sn}_2\text{O}_7$ [17,18], and lifted zero energy modes in $S = 1/2$ kagome systems [19].

This work was made possible by support through the NSF (DMR-0084173 and DMR-0454672), the EIEG program (FSU) and the state of Florida.

*cwiebe@magnet.fsu.edu

- [1] J. E. Greedan, *J. Mater. Chem.* **11**, 37 (2001).
- [2] S. T. Bramwell *et al.*, *Science* **294**, 1495 (2001).
- [3] B. C. den Hertog *et al.*, *Phys. Rev. Lett.* **84**, 3430 (2000).
- [4] S. T. Bramwell *et al.*, *Phys. Rev. Lett.* **87**, 047205 (2001).
- [5] G. C. Lau *et al.*, *Nature Phys.* **2**, 249 (2006).
- [6] A. P. Ramirez *et al.*, *Nature (London)* **399**, 333 (1999).
- [7] L. Pauling, *The Nature of the Chemical Bond* (Cornell Univ. Press, Ithaca, New York, 1945), pp. 301–304.
- [8] P. A. Kozmin *et al.*, *Inorg. Mater.* **33**, 850 (1997).
- [9] K. Matsuhira *et al.*, *J. Phys. Soc. Jpn.* **71**, 1576 (2002).
- [10] J. van Duijn *et al.*, *Phys. Rev. Lett.* **94**, 177201 (2005).
- [11] G. Ehlers *et al.*, *J. Phys. Condens. Matter* **16**, S635 (2004).
- [12] H. Kadowaki *et al.*, *Phys. Rev. B* **65**, 144421 (2002).
- [13] G. Ehlers *et al.*, *J. Phys. Condens. Matter* **15**, L9 (2003).
- [14] J. Snyder *et al.*, *Phys. Rev. Lett.* **91**, 107201 (2003).
- [15] C. Castelnovo *et al.*, *Nature (London)* **451**, 42 (2008).
- [16] J. S. Gardner *et al.*, *Phys. Rev. Lett.* **82**, 1012 (1999).
- [17] I. Mirebeau *et al.*, *Phys. Rev. Lett.* **94**, 246402 (2005).
- [18] F. Bert *et al.*, *Phys. Rev. Lett.* **97**, 117203 (2006).
- [19] K. Matan *et al.*, *Phys. Rev. Lett.* **96**, 247201 (2006).